Predicted Increases in Heat related Mortality under Climate Change in Urban India

Hem H. Dholakia
Vimal Mishra
Amit Garg

W.P. No. 2015-05-02
June 2015

INDIAN INSTITUTE OF MANAGEMENT
AHMEDABAD-380 015
INDIA

Predicted increases in heat related mortality under climate change in urban India

Hem H. Dholakia*[1], Vimal Mishra[2], Amit Garg[1]

Abstract

Mapping mortality impacts of the projected climate in urban areas of developing countries will play a crucial role in instituting planned adaptation measures to protect public health. We provide a comprehensive assessment of mortality in 52 urban areas (population >1 million) that are located in diverse climactic regimes in India. To understand implications of the climate warming on heat wave mortality in the urban India, we used downscaled and bias corrected temperature projections from the Coupled Model Inter-comparison Project Phase 5 (CMIP5) models. Using the observed data for the period of 2005-2012, we developed temperature-mortality relationships using Poisson regression models for the selected urban areas in India. These relationships were applied to future temperature projections from the 23 CMIP5 models for the summer and winter seasons for the Representative Concentration Pathway 4.5 and 8.5 scenarios. Here we show that urban areas in India are projected to witness two-fold or more increases ($p < 0.05$) in heat related mortality (i.e. summer season) under the projected future climate. Mortality is projected to increase 71and 140% in the late 21st century under the RCP 4.5 and 8.5 scenarios, respectively. Moreover, we find that increases in the heat related mortality will overshadow declines in the cold related mortality (winter season). Moreover, urban areas of Delhi, Ahmedabad, Bangalore, Mumbai and Kolkata are projected to experience the highest absolute increases in the heat related mortality in 2080s under the RCP 8.5 scenario. Our findings underscore the need for Indian policy makers to anticipate, plan and respond to the challenge of climate change**.**

[1] **Author affiliations**:

1. Council on Energy, Environment & Water, New Delhi, India
2. Civil Engineering , Indian Institute of Technology, Gandhinagar, India
3. Public Systems Group, Indian Institute of Management, Ahmedabad, India

Author contact information

1. Hem H. Dholakia*
   Council on Energy, Environment and Water, New Delhi; Telephone: +91 1140733365
   Email: hem.dholakia@ceew.in
2. Vimal Mishra
   Indian Institute of Technology Gandhinagar, Chandkheda, Ahmedabad 382424, Gujarat, India
   Telephone: + 91 79 32459904 Email: vmishra@iitgn.ac.in
3. Amit Garg
   Public Systems Group, Indian Institute of Management, Ahmedabad 380015, Gujarat, India;
   Telephone: +91 79 66324952 Email: amitgarg@iimahd.ernet.in

***Corresponding author**: Hem H. Dholakia

Conflicts of interest: None declared

1. Introduction

Extreme temperatures can overwhelm normal functioning of the human body leading to pathological states such as exacerbation of cardiovascular and respiratory disease and ultimately death (Kovats and Hajat 2008). Adverse health effects of temperature extremes are underscored by heatwaves in Europe (Fouillet et al. 2006; Barriopedro et al. 2011), United States (NOAA 2012) and Russia (Barriopedro et al. 2011). Studies have now attributed such episodes and persistently warm seasons to observed climatic warming (Hansen et al. 2012). Furthermore, studies find that the temperature in the near term (i.e. 2040s) will increase despite best mitigation efforts (Coumou and Robinson 2013). Temperature transitions as a result of climate change are likely to leave future populations susceptible to adverse health impacts. These health impacts, however, may dramatically differ across the developed and developing countries (McMichael 2013). Therefore, many researchers have attempted to understand temperature related mortality under the projected future climate.

The clear, consistent finding across studies is that the heat related mortality is set to increase in the future irrespective of location, climate change scenario used, assumptions about temperature mortality relationship, and the period of projections. Reductions in the cold related mortality are expected in future, which may be largely due to a significant reduction in night-time temperatures in urban areas (Mishra et al. 2015). However, it is unlikely that they will completely offset the increase in the heat related deaths (Cheng et al. 2009; Li et al. 2013).

It is observed that almost all studies have assessed impacts for cities or regions in the developed countries such as the United States (Hayhoe et al. 2004; Knowlton et al. 2007), Canada (Cheng et al. 2009; Doyon et al. 2008), Europe (Baccini et al. 2009), and Australia (Huang et al. 2012). Future mortality will largely be determined by the current and future levels of preparedness. Early warning systems and responsive health services in the developed countries may significantly reduce the health impacts; though they are likely to face challenges due to aging population and other socio-economic factors.

India and other developing countries are at higher risk due to high population and low preparedness. Mortality associated with recent heat waves in Indian cities such as Ahmedabad (Singh 2013) and Delhi (Koronowski 2013) highlight the current vulnerability that is likely to increase in the future (Coumou and Robinson 2013). However, studies that assess future temperature related health impacts are largely absent in India (Huang et al. 2011). This is important given that temperatures may increase by 3.3°C to 4.8°C degrees by 2080s relative to pre-industrial times under changing climate (Chaturvedi et al. 2012). Moreover, Kumar et al. (2011) reported that India may experience unprecedented increases in air temperature in the 21^{st} century. Therefore, our understanding of changes in heat waves and its implications on human mortality in the projected future climate in urban India is largely limited. To address this gap, we provide a comprehensive assessment of mortality based on 52 urban areas (population >1 million) located in the diverse climactic regimes across India using downscaled and bias corrected temperature projections from the Coupled Model Inter-comparison Project Phase 5 (CMIP5) models.

2. Data and Methods

As the observed mortality data are not available for all the major urban areas in India, we selected a representative urban area from each climactic regime (BEE 2007) to develop the exposure-response relationships between temperature and mortality (see supplemental material for details). The representative urban areas varied in topography (e.g. plains, coast, and hills) and population characteristics allowing us to map the spatial heterogeneity of climate change and related impacts. Data on daily measurements of air pollution (particulate matter less than 10 microns (PM10), nitrogen oxides and sulphur oxides) were collected from the Central Pollution Control Board (CPCB). Data on daily weather variables (daily maximum and minimum temperature, relative humidity, and dew point temperature) were collected from the India Meteorological Institute (IMD). We collected data on daily totals of registered deaths from the municipal corporations of Ahmedabad, Bangalore, Hyderabad, Lucknow, Mumbai, and Shimla for the period of 2005-2012. The time series estimated for each city differed based on data availability. In most cases, age and cause of death were not available; hence, daily all-cause mortality was studied.

2.1 Temperature mortality relationships

Heat related mortality was estimated for the summer season (March to July) and cold-related mortality was estimated for the winter season (November to February). To model the temperature effects, natural cubic splines with three degrees of freedom were used. It has been argued that using three degrees of freedom captures the short term effect of ambient temperature while leaving out long term and seasonal trends as well as effects of heat or cold waves (Barnett et al. 2012; Rocklov et al. 2012). Within a generalized additive model framework, the regression equation that captures the effect of temperature on mortality can be represented as

$$Log[E(Y_{ij})] = \sum_{j=1}^{P} g\,(x_{ij}) + DOW + \varepsilon \qquad \ldots(1)\ldots$$

where Y_{ij} is the daily number of deaths for the i^{th} city on the j^{th} day and is assumed to follow an over-dispersed Poisson distribution. The covariates x_{ij} represent daily temperature, relative humidity and time for the i^{th} city on the j^{th} day. The effects are expressed by an unknown smooth function g constructed using natural cubic splines. An indicator variable for each day of the week is given by *DOW*. The error term is modeled using ε.

A natural spline with four degrees of freedom for humidity was used. Seasonal and long term trends in data were controlled using a smooth function of time with seven degrees of freedom per year. This is equivalent to a two month moving average which is a good balance between removing long term trends while leaving enough variation to capture short term temperature-mortality relationships (Hajat et al. 2006). This representation has been used is most of the recent studies (Anderson and Bell 2011; Li et al. 2013). Analogous to air pollution, temperature may exhibit delayed effects on mortality and morbidity (Bhaskaran et al. 2013). To capture the delayed effects of temperature an exploratory data analysis was carried out from zero to twenty five day lags. Based upon the statistical analysis and visual inspection of the plots, 0 lags were selected for the hot (summer season) and 2 lags were selected for the cold (winter season).Three alternate model specifications for equation (1) were used in the sensitivity analysis (see supplementary materials).

2.2 Future projections

We obtained daily bias corrected and downscaled projections for daily maximum and minimum temperatures from 23 CMIP5 models. For each of these models, daily projections of minimum and maximum temperature were available up to the year 2100. These projections of temperatures were downscaled and bias corrected for the urban areas using the method described in Thrasher et al., (2012). The modified Bias Correction and Spatial Disaggregation (BCSD) approach (Thrasher et al. 2012) is different from the original BCSD method (Wood et al., 2002; 2004; Maurer et al. 2010) as this uses daily projections of maximum and minimum temperatures rather than monthly average temperatures. The modified BCSD method avoids daily data disaggregation from bias corrected monthly data as used in the original BCSD approach. The bias corrected and spatially disaggregated (BCSD) approach has been used for the hydro-climatic impact assessments (Cayan et al. 2008; Hayhoe et al.

2004; Mishra et al. 2014). Moreover, the BCSD approach has been successfully compared to various downscaling techniques for both mean and extremes climate (Wood et al. 2004; Maurer and Hidalgo 2008; Bürger et al. 2012). Bias-corrected and spatially disaggregated daily dataset were developed for all the selected urban areas considering an overlapping grid cell of 0.5 degree spatial resolution. Using the same approach for the bias correction and downscaling, we developed daily temperature dataset using the CMIP5 model output for the historic period (1950-2005). Our daily projection data are based on statistical downscaling approach; however, data from the dynamical downscaling can be used in future to assess the influence of climate warming on heat wave related mortality.

We considered air temperature projections for the two (4.5 and 8.5) representative concentration pathways (RCP)(Vuuren et al. 2011; Thomson et al., 2011; Riahi et al. 2011). The RCP 4.5 assumes a scenario where radiative forcing stabilizes at 4.5 W/m^2 by the year 2100 (Thomson et al. 2011). This corresponds to an increase in average global temperature of about three degrees centigrade. The RCP 8.5, on the other hand, is an extreme (or worst case) scenario where very little mitigation actions are taken by countries to thwart future climate change. This corresponds to a scenario which has the highest greenhouse gas emissions and may lead to an increase in average temperatures up to six degrees centigrade (Moss et al. 2010; Riahi et al. 2011).

Based on the temperature mortality relationships, deaths for the period from 2000 to 2009 were estimated. The period 2000-2009 was used as the baseline period against which future impacts were compared. Low death registration in Indian cities makes it difficult to find a reliable long-term data on daily deaths (Dhar 2013). The baseline of 2000-2009 roughly corresponds to a period for which mortality data were available. Furthermore, it captures the current climate change impacts and our results portray incremental future changes. Future impacts were compared for the three time periods – the 2020s, the 2050s and the 2080s that roughly correspond to a short, medium and long time horizon.

We used the exposure response relationships to estimate future temperature values. First, based on the shape of the temperature mortality curve (supplementary material Figures S.2 and S.3), a reference temperature that corresponds to minimum mortality was determined. This was called the minimum mortality temperature (MMT). In instances, where the MMT was not clearly discernible from the shape of the graph, the 50th percentile of the temperature distribution was used as the MMT as the risk of mortality at this point was zero (see Supplementary material Table S.5). This approach of comparing the change in relative risks to a minimum mortality temperature has been fairly standard practice in public health (Gosling et al. 2008; Li et al. 2013). Then for each day of the baseline period, the days where the temperature exceeds the MMT were determined. For every day where the temperature exceeded MMT, the relative risk of death was multiplied by average total daily deaths to estimate daily deaths attributable to temperature. The deaths attributable to temperature were summed for all the days from 2000 to 2009 to estimate the baseline mortality. This process was repeated for each day for the future periods – 2020 to 2029, 2050 to 2059 and 2080 to 2089. The total deaths attributable to temperature were estimated for each of the twenty-three climate models, for both RCP scenarios for hot and cold seasons. The difference between future and baseline periods was the excess mortality attributable to temperature. The equation can be represented as –

Mortality = RR x Average daily death rate x Population … (2)…

where

RR: Relative risk based on temperature mortality relationship

Average daily death rate per 1000 population calculated for each city using the SRS estimates

Population – Future population projections are consistent with the shared socioeconomic pathway 4 (SSP) scenarios

The future population projections used was consistent with the Shared Socioeconomic Pathways (SSP) scenarios (O'Neill et al., 2014). The SSPs describe plausible trends in the evolution of society, independent of climate change over the course of the century. We used average population projections of the SSP 4 scenario that envisages a mixed world with rapid technological development in most large countries and lesser development in other portions of the world (O'Neill et al., 2014). Under this scenario, the average population growth for India is about 31% by the year 2050.

It is a well-known that population acclimatize over time to the environmental conditions (Gosling et al. 2008). Therefore to account for the future acclimation, we assumed that populations would acclimatize to 1°C of temperature in every three decades based on the approach used by Dessai (2003). This was incorporated in the analysis by raising the minimum mortality temperature by 1°C for the medium term (the 2050s) and 2°C in the long term (the 2080s). In the short term i.e. the 2020s no acclimatization was assumed.

3. Results

Figure 1 shows current and future seasonal temperature transitions under the projected climate for summer (March to July, Fig 1a-c) and winter (November to February, Fig 1d-f) seasons. During the summer, urban areas are projected to experience average increases in maximum temperature of 1.6°C (95% CI 0.6°C – 2.6°C) and 3°C (95% CI 2°C - 4°C) under

RCP 4.5 (Fig 1b) and RCP 8.5 (Fig 1c), respectively in the 2080s. Under the RCP 8.5, seven urban areas, mostly located in the northern India, will likely experience average increases in maximum temperature of 4°C or more. The average increases in minimum temperature for winter season are 1.8°C (95% CI 0.5°C – 3.1°C) and 3.6°C (95% CI 2.4°C – 4.9°C) under RCP 4.5 (Fig 1e) and RCP 8.5 (Fig 1f), respectively. Twenty urban areas are projected to experience average temperature increases of 4°C or more in winter under the RCP 8.5. These results highlight that urban areas are projected to experience more warming in the winter season than that in the summer. Moreover, urban areas located in the northern India especially in the Gangetic Plain region are projected to face significant warming in the summer and winter seasons.

We observed heterogeneity in the population levels, death rates, and seasonal baseline mortality (Figure 2) across the selected urban areas. It can be noticed that the majority of the selected urban areas fall in the composite climate, while only one urban area was in the temperate climate. Only two urban areas (Shimla and Srinagar) are in the cold climate. Under the RCP 8.5, likely average increases in maximum summer temperatures are 3.3°C (composite zone), 2.7°C (hot and dry zone), 2.3°C (warm and humid zone), 2.7°C (temperate zone) and 4.5°C (cold zone) in the 2080s. These results show that the urban areas in the cold climate are projected to experience the most prominent warming. We find that corresponding statistically significant (p-value < 0.05) increases in heat related mortality (as compared to the baseline) are 84% (composite zone), 150% (hot and dry zone), 127% (warm and humid zone), 107% (temperate zone) and 500% (cold zone), respectively.

For the winter season, the projected average increases in minimum temperature across urban areas are 3.9°C (composite zone), 4°C (hot and dry zone), 2.9°C (warm and humid zone), 2.7°C (temperate zone) and 3.6°C (cold zone) by 2080s under the RCP 8.5 scenario. It can be noticed that the urban areas located in the hot and dry climate are projected to experience the highest increase in minimum temperature. The corresponding percentage decreases in cold related mortality (as compared to the baseline) are 36% (composite zone), 86% (hot and dry zone), 76% (warm and humid zone), 97% (temperate zone) and 75% (cold zone) respectively.

Figure 3 shows the baseline and future transitions of temperature related mortality for the summer and winter seasons across the selected urban areas. Without exception, a clear departure from baseline mortality (Fig 3a) is observed for the summer season (Fig 3b-c), though magnitudes vary across the urban areas. Across all the urban areas, in the 2080s, ~107700 excess heat related deaths are projected under the RCP 4.5 scenario (Fig 3b), which are likely to double (~204900 excess deaths) under the RCP 8.5 scenario (Fig 3c). Winter mortality, for the baseline, is predominantly observed for the urban areas that are located in the Indo-Gangetic Plain (Fig 3d) as compared those located in peninsular India. The likely declines in winter mortality are ~38400 deaths and ~66100 deaths under the RCP 4.5 (Fig 3e) and RCP 8.5 (Fig 3f), respectively.

We show the likely impact of future population growth on projected mortality in Figure 4. Our population projections are based on shared socioeconomic pathway (SSP 4), which is based on a high challenge for adaptation and low challenge for mitigation (O'Neill et al., 2014). The projected number of deaths due to heat are significantly higher ($p < 0.05$) – about 184900 and 318600 excess deaths under the RCP 4.5 and 8.5 respectively. We find that 14 urban areas are likely to have in excess of 5000 deaths compared to the baseline under the RCP 8.5, when we include population projections into consideration. Out of the total selected urban areas, only 9 showed an excess of 5000 deaths compared to baseline when we did not account for population growth. The magnitude of increase highlights the public health significance of temperature related mortality in India. Here it should be noted that these projections of based on a single SSP (SSP4) and these results may vary for the other SSPs. However, our results indicated that the population growth along with the profound warming will pose a serious challenge in heat wave related mortality in India. Moreover, these findings also highlight a need to better understand the climate change, population growth, and mortality linkage in the developing countries that are witnessing a rapid increase in population.

Figure 5 shows the distribution of summer mortality pooled across the selected urban areas before and after accounting for population growth. We find significant differences in the mean ($p<0.05$) and distribution ($p<0.05$) of future mortality under RCP 8.5. We observe a clear rightward shift in the distribution along with an increase in the tail end of the distributions under future climate (Fig 5a). Chennai, Kolkata, and Bangalore are the three urban areas where mortality exceeds the 95th percentile of the baseline distribution. Under the RCP 4.5, additional urban areas that are likely to exceed the 95th percentile include Mumbai, Ahmedabad, Jaipur, and Delhi. Surat is an additional urban area that is likely to exceed the 95th percentile under the RCP 8.5.

From a policy perspective, the five urban areas that will experience the highest increases (supplemental Table S.9) in the future heat related mortality after accounting for population increase are Delhi (Δ 15200 deaths) , Ahmedabad (Δ 17600 deaths), Bangalore (Δ 14900 deaths), Kolkata (Δ 19400 deaths) and Mumbai (Δ 15300 deaths). Of these, Ahmedabad is the only urban area that has recently instituted a heat-health warning system (AMC 2013) thereby underscoring the need to institute planned adaptation measures for other urban areas.

4. Discussion and Conclusions

Our findings showed that the average percentage increase in heat-related mortality in 2080s for RCP 8.5 across different models is 140±37% as compared to the baseline. The corresponding percentage decline in cold –related mortality is 69±10%. Across the different zones studied, we find that maximum percentage increases in the heat related mortality are expected in the cold zone and hot and dry zone. This may be because people in the colder areas may not acclimatize to warmer temperatures. Similarly, increased temperatures in the zones that are hot and dry may enhance population susceptibility given that physiological limits of human temperature tolerance may be breached (Kovats & Hajat, 2008). Declines in cold related mortality with increasing temperature have received lesser attention though average winter temperatures are correlated with excess winter deaths in Europe (Healy, 2003). We find heterogeneity in increases in minimum temperature and corresponding declines in cold related mortality. The differences across climate zones may be explained in part by differing levels of acclimatization. This, however, remains an important area of study.

The real mortality impact of the projected climate in urban areas in India is likely to be significantly higher than that analyzed in this study. The 52 urban areas we studied represent about 13% (~157 million people) of the Indian population. The remaining population that resides in smaller towns, cities, and rural areas, which are also vulnerable to mortality impacts of climate change. The towns and smaller cities of today will burgeon into urban areas with million plus populations in the future as a consequence of urbanization. Therefore, the health impacts may be higher than what we have estimated. The strength of this study is that although our findings may be underestimates, they are significant enough to warrant the attention of policy makers.

The direction of our results i.e. increases in temperature related mortality is comparable to the previous studies (Li et al. 2013; Hayhoe et al. 2004; Knowlton et al. 2007). For instance, a recent study of New York, found that net increases in mortality in the 2080s was expected to be 15.5% and 31% under the B1 and A2 SRES scenarios respectively (Li et al. 2013). Their study applied exposure-response relationships to results from 16 regionally downscaled models although it did not account for future acclimatization. Hayhoe et al. (2004) estimated a two to three-fold increase in the heat related mortality by 2090s in the state of California under the A1and B1 SRES scenarios (Hayhoe et al. 2004). However, urban areas in developed countries have better infrastructure, higher incomes, better governance, and more responsive health systems and thus better poised to respond to health challenges. Developing countries are significantly more vulnerable as impacts may not only be higher in absolute terms but also because they lack resources to mount a coherent adaptation response (Smith et al. 2014).

Our study does not take into account how mortality will change in the future depending on factors (e.g. heat island effects, migration, behavior patterns) other than those we have controlled for (i.e. temperature, humidity, and pollution). This is because it is difficult to project mortality rates in a robust manner. Changes in the age structure of populations may expose a larger group of elderly people and enhance vulnerability to temperature related mortality risk (Huang et al. 2011). Furthermore, urbanization patterns may contribute to urban heat island effects that may enhance temperature related mortality risk (Stone et al. 2010). On the other hand, benefits of increased incomes due to economic growth, education, poverty reduction and better health systems may offer significant protection against temperature related mortality. Thus, future mortality changes will be an outcome of the complex interaction of the aforementioned factors.

Another important point is that our study does not take into account the impacts of future planned adaptation measures. Economic growth, early warning systems, access to air conditioning and heating systems, behavioral change in communication and other adaptation measures could potentially reduce temperature related mortality (Toloo et al. 2013; Ebi and Burton 2008; Frumkin et al. 2008). However, building the future scenarios to project the benefits of adaptation is complex because adaptation measures are likely to be very specific to individuals or communities. In addition, studies that quantify the benefits of current adaptation measures in the health sector are largely absent. Therefore, we adopted a modified exposure – response curve approach used previously (Dessai 2003) to account for physiologic acclimatization. Other approaches to capturing acclimatization such as 'analog city' (Knowlton et al. 2007) have received much criticism (Gosling et al. 2008) and, therefore, have been avoided.

Mortality reductions due to acclimatization are highly variable and are sensitive to the climate zone, time period, and climate change scenario. For the RCP 8.5 in the long term (2080s) acclimatization effects range from 4% to 12% in the summer season and 1% to 10% in the winter season. Previous studies have found higher acclimatization effects - likely mortality reductions of 25% in New York City (Knowlton et al. 2007) and 15-20% reduction in California (Hayhoe et al. 2004). These differences in the magnitude of change are driven by the choice of methodology and the direction of change may be more important to understand.

Application of exposure mortality relationships from one city to other cities in the same climate zone, as we do here, implicitly assumes that demographic structure, population exposure, and particulate matter concentrations are similar. Furthermore, it assumes that future development pathways will be more or less similar. However, given that different urban areas show different development patterns, vulnerability profiles across cities within the same climate zone may vary considerably. Thus, while highly uncertain, the estimation of health impacts should be viewed as indicative of the direction of future transitions relative to the current scenario.

Typically, future projections are marred by large uncertainties from a variety of sources such as uncertainties in emission scenarios, downscaling procedures, temperature mortality relationships, population transitions and future adaptation (Gosling et al. 2008). However, very often in large scale integrated modeling exercises it is not always possible to quantify these uncertainties (Amann et al. 2011). Nonetheless, we attempted to minimize these uncertainties to the extent possible. A large number of alternate models have been evaluated and a sensitivity analysis (supplementary material Tables S.3 & S.4) has been undertaken to develop a core model for temperature mortality relationships. In addition, we studied twenty three downscaled climate models respectively to account for uncertainty within and across models. The two emission scenarios – RCP 4.5 and RCP 8.5 capture a large range of future temperature transitions from current temperature trajectory to an extreme degree of global warming, thereby addressing a vast range of uncertainty with respect to future climate.

A key limitation of this study is that we use only seven years of observed mortality data to develop temperature-mortality relationships. Previous studies have used 15 to 20 years of observed data to develop temperature-mortality relationships for carrying out future projections (Li et al. 2013; Knowlton et al. 2007). However, these studies have been confined to developed countries where vital registration systems are vastly better than those in developing countries such as India. Therefore, this study underscores the need for collecting quality data so that evidenced based adaptation policy measures can be developed. In conclusion, this is the first attempt to show that urban India is projected to experience high mortality from the future warming. Our findings underscore the need for Indian policy makers to anticipate, plan and respond to the challenge of climate change. The heat action plan of Ahmedabad (AMC 2013) as well as the state level action plans on climate change (MoEF 2014) are indicative of initial forays being made on this front. However, a greater emphasis on public health, policy coordination across sectors along with health system strengthening is needed in urban India to address current and future climate change related health challenges.

Acknowledgement:

The authors declare no competing financial interests. The authors wish to acknowledge Reepal Shah for research assistance in preparing this manuscript. The second author appreciates funding from the Varahamihir Research Fellowship from the Indian Ministry of Earth Sciences. The authors acknowledge constructive comments from the three reviewers that helped to improve the manuscript.

References

Amann, M., and Coauthors, 2011: Cost-effective control of air quality and greenhouse gases in Europe: Modeling and policy applications. *Environ. Model. Softw.*, **26**, 1489–1501, doi:10.1016/j.envsoft.2011.07.012.

AMC, 2013: *Ahmedabad heat action plan*. Ahmedabad Municipal Corporation, Ahmedabad, http://www.egovamc.com/downloads/healthcare/healthpdf/heat_action_plan.pdf (Accessed September 29, 2013).

Anderson, G. B., and M. L. Bell, 2011: Heat waves in the United States: mortality risk during heat waves and effect modification by heat wave characteristics in 43 US communities. *Environ. Health Perspect.*, **119**, 210.

Baccini, M., and Coauthors, 2009: Impact of heat on mortality in 15 European cities: attributable deaths under different weather scenarios. *J. Epidemiol. Community Health*, **65**, 64–70, doi:10.1136/jech.2008.085639.

Barnett, A. G., S. Hajat, A. Gasparrini, and J. Rocklöv, 2012: Cold and heat waves in the United States. *Environ. Res.*, **112**, 218–224, doi:10.1016/j.envres.2011.12.010.

Barriopedro, D., E. M. Fischer, J. Luterbacher, R. M. Trigo, and R. Garcia-Herrera, 2011: The Hot Summer of 2010: Redrawing the Temperature Record Map of Europe. *Science*, **332**, 220–224, doi:10.1126/science.1201224.

BEE, 2007: *Energy Conservation Building Code*. Bureau of Energy Efficiency, Government of India, New Delhi, http://high-performancebuildings.org/about.php (Accessed November 21, 2014).

Bhaskaran, K., A. Gasparrini, S. Hajat, L. Smeeth, and B. Armstrong, 2013: Time series regression studies in environmental epidemiology. *Int. J. Epidemiol.*, doi:10.1093/ije/dyt092. http://www.ije.oxfordjournals.org/cgi/doi/10.1093/ije/dyt092 (Accessed August 21, 2013).

Bürger, G., T. Q. Murdock, A. T. Werner, S. R. Sobie, and A. J. Cannon, 2012: Downscaling Extremes—An Intercomparison of Multiple Statistical Methods for Present Climate. *J. Clim.*, **25**, 4366–4388, doi:10.1175/JCLI-D-11-00408.1.

Cayan, D. R., E. P. Maurer, M. D. Dettinger, M. Tyree, and K. Hayhoe, 2008: Climate change scenarios for the California region. *Clim. Change*, **87**, 21–42, doi:10.1007/s10584-007-9377-6.

Chaturvedi, R., J. Joshi, M. Jayaraman, G. Bala, and N. Ravindranath, 2012: Multi-model climate change projections for India under representative concentration pathways. *Curr. Sci.*, **103**, 791–802.

Cheng, C. S., and Coauthors, 2009: Differential and combined impacts of extreme temperatures and air pollution on human mortality in south–central Canada. Part II: future estimates. *Air Qual. Atmosphere Health*, **1**, 223–235, doi:10.1007/s11869-009-0026-2.

Coumou, D., and A. Robinson, 2013: Historic and future increase in the global land area affected by monthly heat extremes. *Environ. Res. Lett.*, **8**, 034018, doi:10.1088/1748-9326/8/3/034018.

Dessai, S., 2003: Heat stress and mortality in Lisbon Part II. An assessment of the potential impacts of climate change. *Int. J. Biometeorol.*, **48**, 37–44, doi:10.1007/s00484-003-0180-4.

Dhar, A., 2013: Birth and death registration still low in India. *The Hindu*, April 18 http://www.thehindu.com/news/national/births-and-deaths-registration-still-low-in-india/article4630425.ece (Accessed November 17, 2013).

Doyon, B., D. Bélanger, and P. Gosselin, 2008: The potential impact of climate change on annual and seasonal mortality for three cities in Québec, Canada. *Int. J. Health Geogr.*, **7**, 23, doi:10.1186/1476-072X-7-23.

Ebi, K. L., and I. Burton, 2008: Identifying practical adaptation options: an approach to address climate change-related health risks. *Environ. Sci. Policy*, **11**, 359–369, doi:10.1016/j.envsci.2008.02.001.

Fouillet, A., and Coauthors, 2006: Excess mortality related to the August 2003 heat wave in France. *Int. Arch. Occup. Environ. Health*, **80**, 16–24.

Frumkin, H., J. Hess, G. Luber, J. Malilay, and M. McGeehin, 2008: Climate change: the public health response. *Am. J. Public Health*, **98**, 435–445.

Gosling, S. N., J. A. Lowe, G. R. McGregor, M. Pelling, and B. D. Malamud, 2008: Associations between elevated atmospheric temperature and human mortality: a critical review of the literature. *Clim. Change*, **92**, 299–341, doi:10.1007/s10584-008-9441-x.

Hajat, S., R. S. Kovats, and K. Lachowycz, 2006: Heat-related and cold-related deaths in England and Wales: who is at risk? *Occup. Environ. Med.*, **64**, 93–100, doi:10.1136/oem.2006.029017.

Hansen, J., M. Sato, and R. Ruedy, 2012: Perception of climate change. *Proc. Natl. Acad. Sci.*, **109**, E2415–E2423.

Hayhoe, K., and Coauthors, 2004: Emissions pathways, climate change, and impacts on California. *Proc. Natl. Acad. Sci. U. S. A.*, **101**, 12422–12427.

Healy, J. D., 2003: Excess winter mortality in Europe: a cross country analysis identifying key risk factors. *J Epidemiol. Community Health*, **57**, 784–789.

Huang, C., A. G. Barnett, X. Wang, P. Vaneckova, G. FitzGerald, and S. Tong, 2011: Projecting Future Heat-Related Mortality under Climate Change Scenarios: A Systematic Review. *Environ. Health Perspect.*, **119**, 1681–1690, doi:10.1289/ehp.1103456.

——, A. G. Barnett, X. Wang, and S. Tong, 2012: The impact of temperature on years of life lost in Brisbane, Australia. *Nat. Clim. Change*, **2**, 265–270, doi:10.1038/nclimate1369.

Knowlton, K., B. Lynn, R. A. Goldberg, C. Rosenzweig, C. Hogrefe, J. K. Rosenthal, and P. L. Kinney, 2007: Projecting heat-related mortality impacts under a changing climate in the New York City region. *J. Inf.*, **97**. http://ajph.aphapublications.org/doi/abs/10.2105/AJPH.2006.102947 (Accessed April 27, 2013).

Koronowski, R., 2013: Intense Heat Wave In India Brings Sunstroke Deaths, Electric Grid Meltdown, And Spoiled Fruit. *Clim. Prog.*,. http://thinkprogress.org/climate/2013/05/29/2076071/intense-heat-wave-in-india-brings-sunstroke-deaths-electric-grid-meltdown-and-spoiled-fruit/ (Accessed December 16, 2013).

Kovats, R. S., and S. Hajat, 2008: Heat Stress and Public Health: A Critical Review. *Annu. Rev. Public Health*, **29**, 41–55, doi:10.1146/annurev.publhealth.29.020907.090843.

Li, T., R. M. Horton, and P. L. Kinney, 2013: Projections of seasonal patterns in temperature- related deaths for Manhattan, New York. *Nat. Clim. Change*, doi:10.1038/nclimate1902. http://www.nature.com/doifinder/10.1038/nclimate1902 (Accessed May 22, 2013).

Maurer, E. P., and H. G. Hidalgo, 2008: Utility of daily vs. monthly large-scale climate data: an intercomparison of two statistical downscaling methods. *Hydrol. Earth Syst. Sci.*, **12**, 551–563.

McMichael, A. J., 2013: Globalization, Climate Change, and Human Health. *N. Engl. J. Med.*, **368**, 1335–1343, doi:10.1056/NEJMra1109341.

Mishra, V., R. Shah, and B. Thrasher, 2014: Soil moisture droughts under retrospective and projected climate in India. *J. Hydrometeorol.*, doi:10.1175/JHM-D-13-0177.1.

MoEF, 2014: State action plan on climate change. *Minist. Environ. For. Gov. India*,. http://envfor.nic.in/ccd-sapcc (Accessed January 31, 2014).

Moss, R. H., and Coauthors, 2010: The next generation of scenarios for climate change research and assessment. *Nature*, **463**, 747–756, doi:10.1038/nature08823.

NOAA, 2012: *State of the Climate: Wildfires for August 2012*. National Oceanic and Atmospheric Administration, Asheville, NC, http://www.ncdc.noaa.gov/sotc/fire/2012/8 (Accessed September 23, 2014).

O'Neill, B. C., and Coauthors, 2014: A new scenario framework for climate change research: the concept of shared socioeconomic pathways. Climatic Change, 122, 387–400, doi: 10.1007/s10584-013-0905-2.

Riahi, K., and Coauthors, 2011: RCP 8.5—A scenario of comparatively high greenhouse gas emissions. *Clim. Change*, **109**, 33–57, doi:10.1007/s10584-011-0149-y.

Rocklov, J., A. G. Barnett, and A. Woodward, 2012: On the estimation of heat-intensity and heat-duration effects in time series models of temperature-related mortality in Stockholm, Sweden. *Environ. Health*, **11**, 1–12.

Singh, J., 2013: Ahmedabad's beat-the-heat plan. *Earth*,. http://www.downtoearth.org.in/content/ahmedabad-s-beat-heat-plan (Accessed December 20, 2013).

Smith, K. R., and Coauthors, 2014: Human Health: Impacts, Adaptation and Co-benefits. *Climate Change 2014: Impacts, Adaptation and Vulnerability*, Intergovernmental Panel on Climate Change, Geneva.

Stone, B., J. J. Hess, and H. Frumkin, 2010: Urban Form and Extreme Heat Events: Are Sprawling Cities More Vulnerable to Climate Change Than Compact Cities? *Environ. Health Perspect.*, **118**, 1425–1428, doi:10.1289/ehp.0901879.

Thomson, A. M., and Coauthors, 2011: RCP4.5: a pathway for stabilization of radiative forcing by 2100. *Clim. Change*, **109**, 77–94, doi:10.1007/s10584-011-0151-4.

Thrasher, B., E. P. Maurer, C. McKellar, and P. B. Duffy, 2012: Technical Note: Bias correcting climate model simulated daily temperature extremes with quantile mapping. *Hydrol Earth Syst Sci*, **16**, 3309–3314, doi:10.5194/hess-16-3309-2012.

Toloo, G., G. FitzGerald, P. Aitken, K. Verrall, and S. Tong, 2013: Evaluating the effectiveness of heat warning systems: systematic review of epidemiological evidence. *Int. J. Public Health*, **58**, 667–681, doi:10.1007/s00038-013-0465-2.

Vuuren, D. P., and Coauthors, 2011: The representative concentration pathways: an overview. *Clim. Change*, **109**, 5–31, doi:10.1007/s10584-011-0148-z.

Wood, A. W., L. R. Leung, V. Sridhar, and D. P. Lettenmaier, 2004: Hydrologic Implications of Dynamical and Statistical Approaches to Downscaling Climate Model Outputs. *Clim. Change*, **62**, 189–216, doi:10.1023/B:CLIM.0000013685.99609.9e.

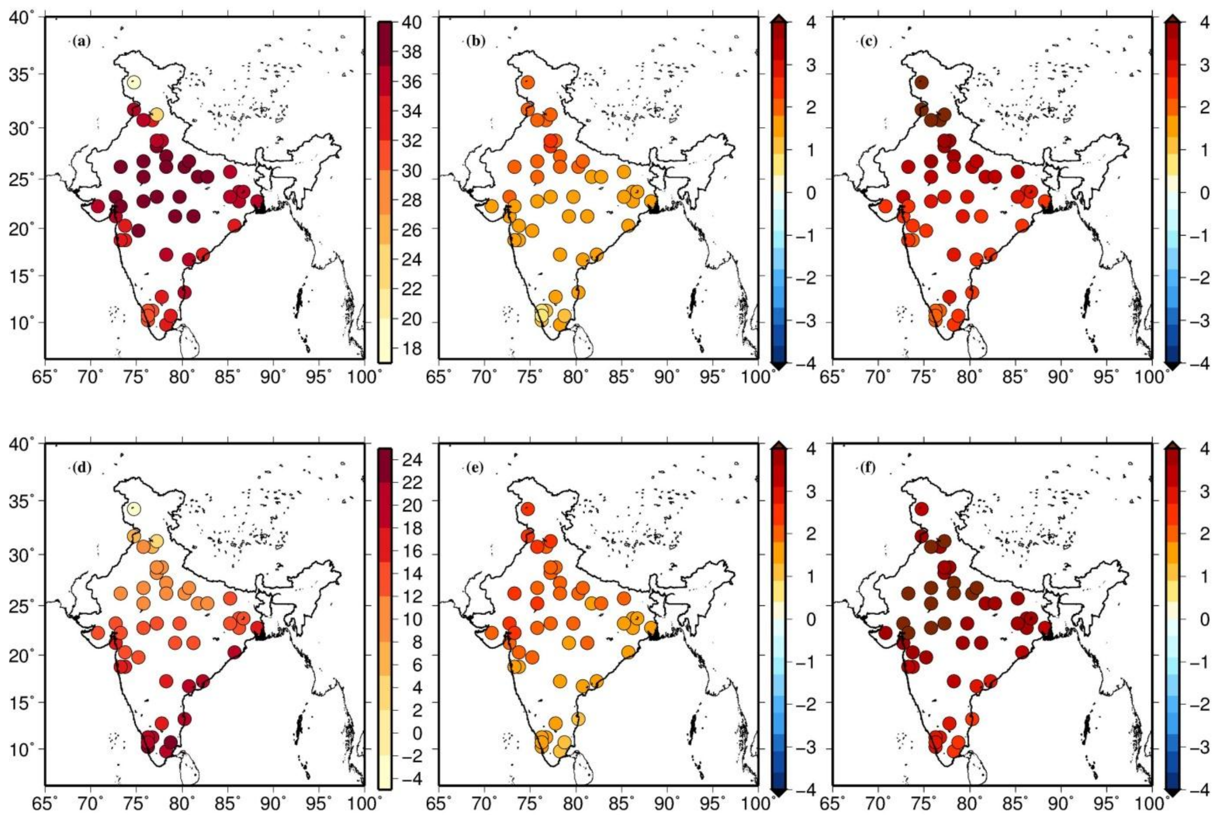

Figure 1. (a) Baseline (2000 – 2009) maximum temperature (°C) during the summer months (March to July); (b) change in temperatures (°C) under RCP 4.5 in 2080s, and (c) under RCP 8.5 in 2080s, (d) Baseline minimum temperature (°C) during the winter months (November to February), (e) change in winter temperatures (°C) under RCP 4.5 in 2080s, and (f) RCP 8.5 in 2080s. Every circle represents an urban area with million plus population. Colours distinguish urban area by baseline temperature values. Maps were created by authors using the GMT software.

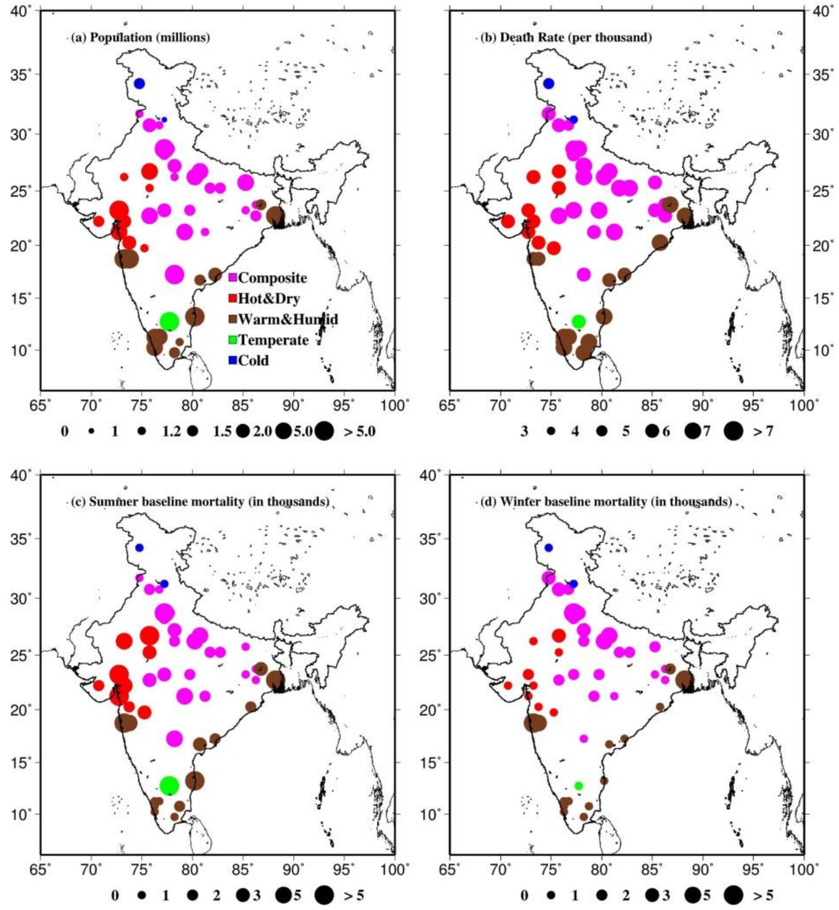

Figure 2. (a) Population (in millions) based on 2011 Census, (b) Annual crude death rate (per 1000 population) in 2011, (c) baseline mortality in summer season (March – July), (d) baseline mortality in winter season (November – February). Every circle represents an urban area with million plus population. Colours distinguish urban area by climate regimes – pink for composite zone, blue for cold zone, brown for warm and humid zone, green for temperate zone and red for hot & dry zone.

Maps were created by authors using the GMT software.

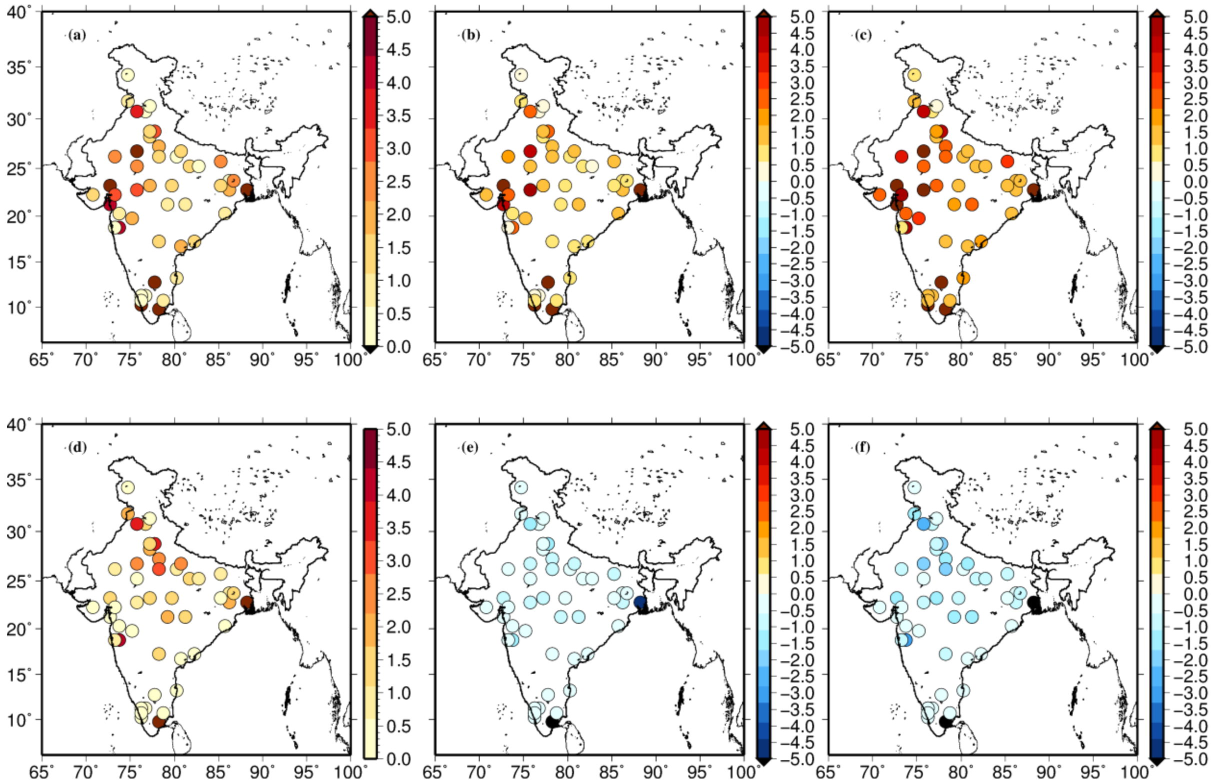

Figure 3. (a) Baseline (2000 - 2009) mortality (in thousands) during the summer months (March to July); (b) change in mortality under RCP 4.5 in 2080s, and (c) under RCP 8.5 in 2080s, (d) Baseline mortality (in thousands) during the winter months (November to February), (e) change in mortality under RCP 4.5 in 2080s, and (f) under RCP 8.5 in 2080s. Every circle represents an urban area with million plus population.

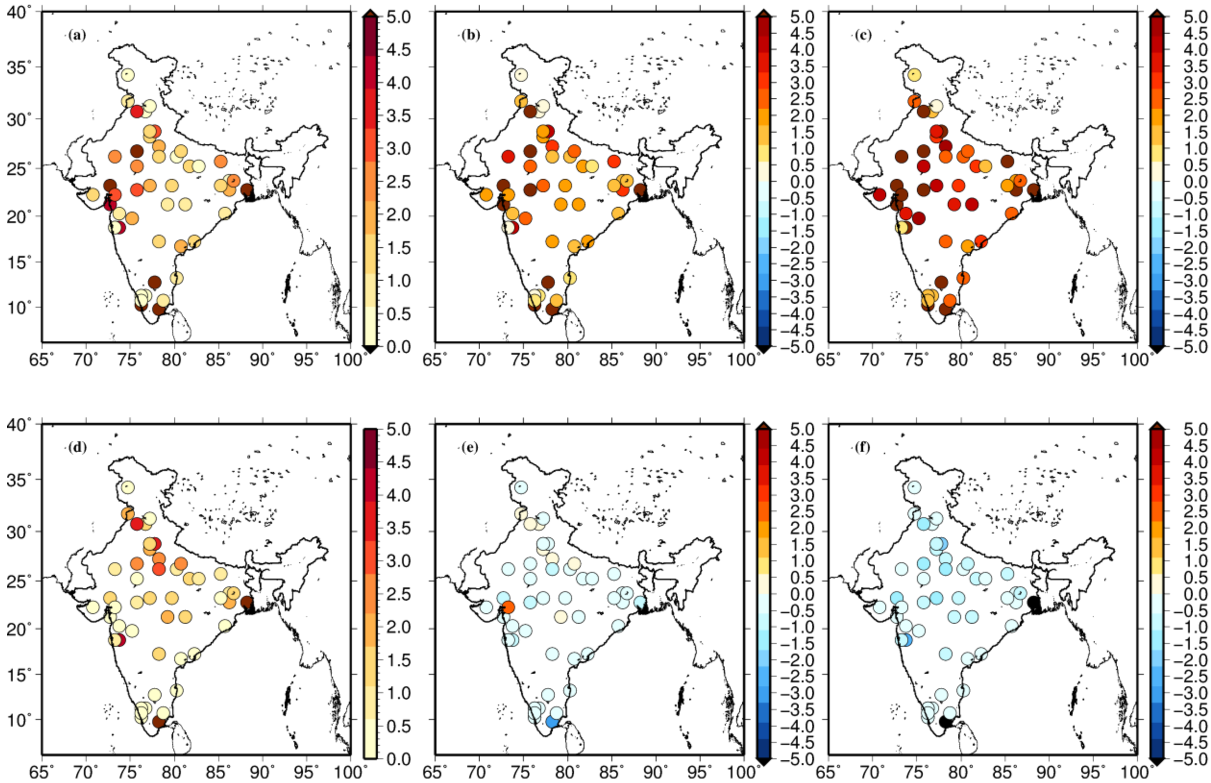

Figure 4. (a) Baseline (2000 – 2009) mortality (in thousands) during the summer months (March to July) after accounting for future population growth (consistent with SSP 4); (b) change in summer mortality under RCP 4.5 in 2080s, and (c) under RCP 8.5 in 2080s, (d) Baseline mortality (in thousands) during the winter months (November to February) after accounting for future population growth, (e) change in winter mortality under RCP 4.5 in 2080s, and (f) under RCP 8.5 in 2080s. Every circle represents an urban area with million plus population.

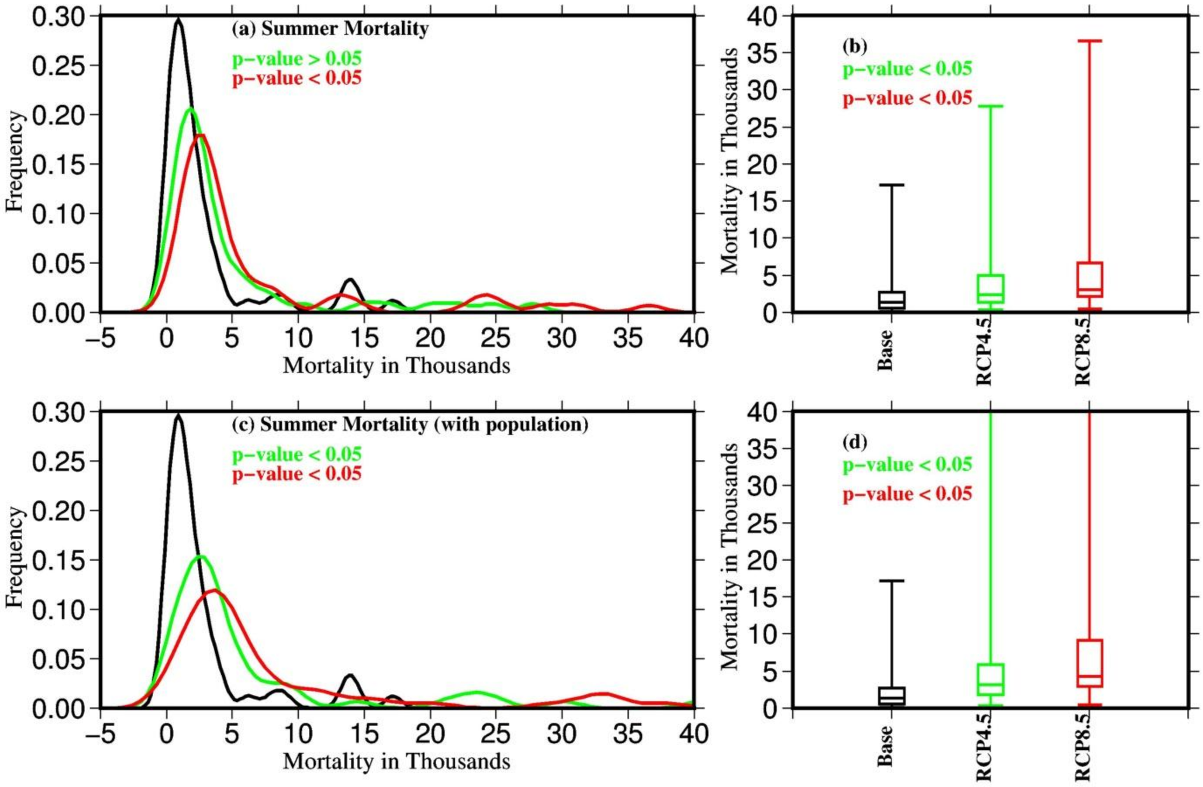

Figure 5. (a, b) Distribution and box plot of heat related mortality for baseline (black line), RCP 4.5 (green line) and RCP 8.5 (red line), (c, d) same as (a, b) after accounting for future population growth. Changes and their statistical significance (at 5% level) were estimated using the Ranksum test (for mean) and Kolmogorov-Smirnov test (for distribution).

SUPPLEMENTARY MATERIAL

Predicted increases in heat related mortality under climate change in urban India

Hem H. Dholakia[1], Vimal Mishra[2], Amit Garg[1]

1. Public Systems Group, Indian Institute of Management, Ahmedabad, India
2. Civil Engineering Department, Indian Institute of Technology, Gandhinagar, India

Selection of Cities

Figure S.1 Map of India showing locations of Cities in this study (Dholakia, Bhadra & Garg, 2014)

Table S.1 Representative Cities by climate zone

Climate zone	Representative city	Topography
Hot and dry	Ahmedabad	Plains
Cold	Shimla	Hilly regions
Temperate	Bangalore	Plateau
Composite	Hyderabad	Plains
Warm and humid	Mumbai	Coastal areas

India is divided into five climate zones namely – hot and dry, warm and humid, composite, temperate and cold. The rationale for choosing these cities was that they are each representative of a different climate zone in India. In addition to climate zone, these cities represent varied topography – plains, plateau, coastal areas and hilly regions. Though climate change is a global phenomenon, its impacts are local in nature and are likely to vary across cities and climate zones. Therefore cities were selected such that they broadly represent varying vulnerability to climate change related impacts.

Air pollution data

Data on daily measurements of air pollution were collected from the Central Pollution Control Board (CPCB). The CPCB has set up the National Ambient Air Quality Monitoring Program (NAMP). Under the NAMP, four criteria pollutants i.e. Sulphur Dioxide (SO_2), Oxides of Nitrogen (NO_x), Total suspended particles (TSP) and Particulate matter less than 10 microns (PM_{10}) are measured for 342 stations located in 127 cities across India. On an average 100 - 120 measurements per year (i.e. about 2 per week) are taken for each station and the values reported are a 24-hour average.

Mortality data

Mortality data in India comes from two sources. The first source is the Sample Registration Survey (SRS) carried out by the Office of the Registrar General of India. The SRS reports annual crude birth and death rates as well as infant mortality rates for urban and rural areas for all Indian states and Union Territories. Initiated in 1964-65, it became fully operational in 1969 and today covers 7957 sample units which is about 7.35 million population (RGI, 2012).

The second source is the Municipal corporations that register daily births and deaths taking place within their administrative boundaries. This includes births and deaths taking place at home and within hospitals. Ideally, information related to mortality should capture age, gender and cause of death according to the International Classification of Disease (ICD – 10) as prescribed by the World Health Organization (WHO, 2010).

If birth and death registration systems manage to capture all births and deaths then the numbers from both sources (SRS & Municipal Corporations) should be similar. However, in developing countries such as India it rarely happens that all births and deaths are registered. Sometimes even if deaths do get registered, information on age or cause of death may not get recorded. For this study we collected the daily total of registered deaths in the municipal corporations of Ahmedabad, Bangalore, Hyderabad, Lucknow, Mumbai and Shimla. In most cases, age distributions and cause of death were not available. Hence, daily all-cause mortality was studied.

Table S.2 Comparison of SRS estimates and values recorded from Municipal Corporation

City	Annual deaths as per SRS	Registered Deaths in MC	Absolute Difference	% Shortfall vs. SRS
Ahmedabad	36206	39748	-3542	0
Bangalore	45895	45692	203	0.4
Hyderabad	40295	21602	18693	46.4
Mumbai	93911	80922	12989	13.8
Shimla	612	1781	-1169	0

Table S.2 shows that there is a difference between the SRS estimates and the deaths registered in the Municipal corporations. This difference was highest for Hyderabad where the data recorded from the corporation were 46.4% less as compared to the SRS estimates. Ahmedabad, Bangalore and Shimla did not show any differences between recorded deaths and SRS estimates.

Reconciliation between the municipal recorded deaths and the SRS is often difficult as a one-is-to-one mapping between the two data sources is not possible. However, the comparison allows for identification of any gross under - reporting of deaths that might take place. The daily deaths collected from the municipal corporation represent the best available data and have been used in the study.

Weather data

Data on daily weather variables were collected from the Indian Meteorological Institute (IMD). The IMD has a record of daily weather variables since the year 1948. The weather variables studied included daily maximum and minimum temperature, relative humidity and dew point temperature.

Modelling Paradigm

To model the temperature effects, natural cubic splines with three degrees of freedom were used. It has been argued that using three degrees of freedom captures the short term effect of ambient temperature while leaving out long term and seasonal trends as well as effects of heat or cold waves (Barnett et al., 2012; Rocklov et al., 2012). Within a generalized additive model framework, the regression equation that captures the effect of temperature on mortality can be represented as

$$Log[E(Y_{ij})] = \sum_{j=1}^{P} g\ (x_{ij}) + DOW + \varepsilon \qquad \ldots(1)\ldots$$

where Y_{ij} is the daily number of deaths for the i^{th} city on the j^{th} day and is assumed to follow an over-dispersed Poisson distribution. The covariates x_{ij} represent daily temperature, relative humidity and time for the i^{th} city on the j^{th} day. The effects are expressed by an unknown smooth function g constructed using natural cubic splines. An indicator variable for each day of week is given by *DOW*. The error term is modelled using ε.

A natural spline with four degrees of freedom for humidity was used. Seasonal and long term trends in data were controlled for using a smooth function of time with seven degrees of freedom per year. This is equivalent to a two month moving average and is thought be a good balance between removing long term trends while leaving enough variation to capture short term temperature- mortality relationships (Hajat et al., 2006).This representation has been used is most of the recent studies (Anderson & Bell, 2011; Li et al., 2013).

Analogous to air pollution, temperature may exhibit delayed effects on mortality and morbidity (Bhaskaran et al., 2013). To capture the delayed effects of temperature an exploratory data analysis was carried out from zero to twenty five lags. Based upon statistical analysis and visual inspection of the plots, 0 lags were selected for the hot (summer season) and 2 lags were selected for the cold (winter season).

There is no standard way to measure the heat (or cold) effect and other researchers have used alternate measures. For instance, Anderson & Bell (2009) measure the heat effect as the difference between relative risk at 99^{th} percentile and 90^{th} percentile of temperature distribution. Since we were interested in the changes in mortality closer to the extremes of the temperature distribution, the heat effect was defined as the percentage change in mortality between the 99th percentile and 95th percentile of the temperature distribution as suggested by Li et al. (2013).

$$\text{Heat effect} = \frac{\text{Relative risk at } 99^{th} \text{ percentile} - \text{Relative risk at } 95^{th} \text{ percentile}}{\text{Relative risk at } 95^{th} \text{ percentile}} \quad \ldots(2)\ldots$$

Similarly, the cold effect was defined as the percentage change in mortality between the 1st and 5th percentile of the temperature distribution. These definitions of heat and cold effect have been previously used in the literature (Li et al., 2013).

$$\text{Cold effect} = \frac{\text{Relative risk at } 1^{st} \text{ percentile} - \text{Relative risk at } 5^{th} \text{ percentile}}{\text{Relative risk at } 5^{th} \text{ percentile}} \quad \ldots(3)\ldots$$

A sensitivity analysis of the core model presented in equation (1) was undertaken. Three alternate model specifications were used in the sensitivity analysis. The first alternate model included pollution as a confounding variable; the second used dew point temperature instead of humidity and the final model included pollution with the assumption that standards set by the World Health Organization were met.

Table S.3 Heat effect (%) for different models across cities

City	Core Model	Dew Point	Air Pollution	WHO	Lag 2
Ahmedabad	6.56	6.98	4.45	6.60	7.9
95% CI	*(4.84, 8.31)*	*(5.18, 8.81)*	*(0.97, 8.04)*	*(4.88, 8.35)*	*(5.87, 9.97)*
Bangalore	3.69	3.09	3.59	3.78	3.77
95% CI	*(1.38, 6.04)*	*(0.82, 5.41)*	*(-0.66, 8.02)*	*(1.48, 6.13)*	*(0.65, 6.97)*
Hyderabad	5.06	5.27	4.87	5.09	4.39
95% CI	*(1.71, 8.51)*	*(1.89, 8.77)*	*(0.87, 9.04)*	*(1.72, 8.57)*	*(1.47, 7.4)*
Mumbai	3.53	2.68	3.77	3.47	3.59
95% CI	*(1.69, 5.4)*	*(0.87, 4.53)*	*(1.91, 5.65)*	*(1.65, 5.33)*	*(0.72, 6.59)*
Shimla	8.11	na	18.25	8.56	9.5
95% CI	*(0.99, 15.73)*		*(2.75, 36.1)*	*(1.41, 16.21)*	*(1.87, 17.71)*

These values show the change in relative risk of mortality when temperature increases from 95^{th} to 99^{th} percentile of the temperature distribution in the summer season for a given city
NA – no humidity or dew point data available for Shimla

Table S.4 Cold effect (%) for different models across cities

City	Core Model	Dew Point	Air Pollution	WHO
Ahmedabad	7.09	8.91	8.23	7.11
95% CI	*(4.3, 9.96)*	*(5.93, 11.97)*	*(4.02, 12.61)*	*(4.32, 9.98)*
Bangalore*	1.15	0.84	-1.3	1.23
95% CI	*(-1.47, 3.84)*	*(-1.77, 3.53)*	*(-7.85, 5.71)*	*(-1.41, 3.93)*
Hyderabad*	1.79	2	2.71	2.01
95% CI	*(1.21, 4.88)*	*(-1.11, 5.2)*	*(-1.03, 6.59)*	*(-1.01, 5.11)*
Mumbai	5.33	5.94	5.69	5.37
95% CI	*(2.6, 8.12)*	*(2.95, 9.01)*	*(2.45, 9.04)*	*(2.64, 8.17)*
Shimla	0.93	na	-7.55	0.61
95% CI	*(-5.25, 7.51)*		*(-20.06, 6.91)*	*(-5.54, 7.21)*

These values show the change in relative risk of mortality when temperature decreases from 5^{th} to 1^{st} percentile of the temperature distribution in the winter season for a given city. *Cold effect at lag zero; ** at lag 1. For all other cities at lag 2 of temperature
NA – no humidity or dew point data available for Shimla

Table S.5 Minimum mortality temperature for hot and cold seasons

City	Hot season (maximum temperature)	Cold season (minimum temperature)
Ahmedabad	32.2°C	17.8°C
Bangalore	27.8°C	16.8°C
Hyderabad	36.5°C	18°C
Mumbai	30.9°C	20.6°C
Shimla	20°C	3°C

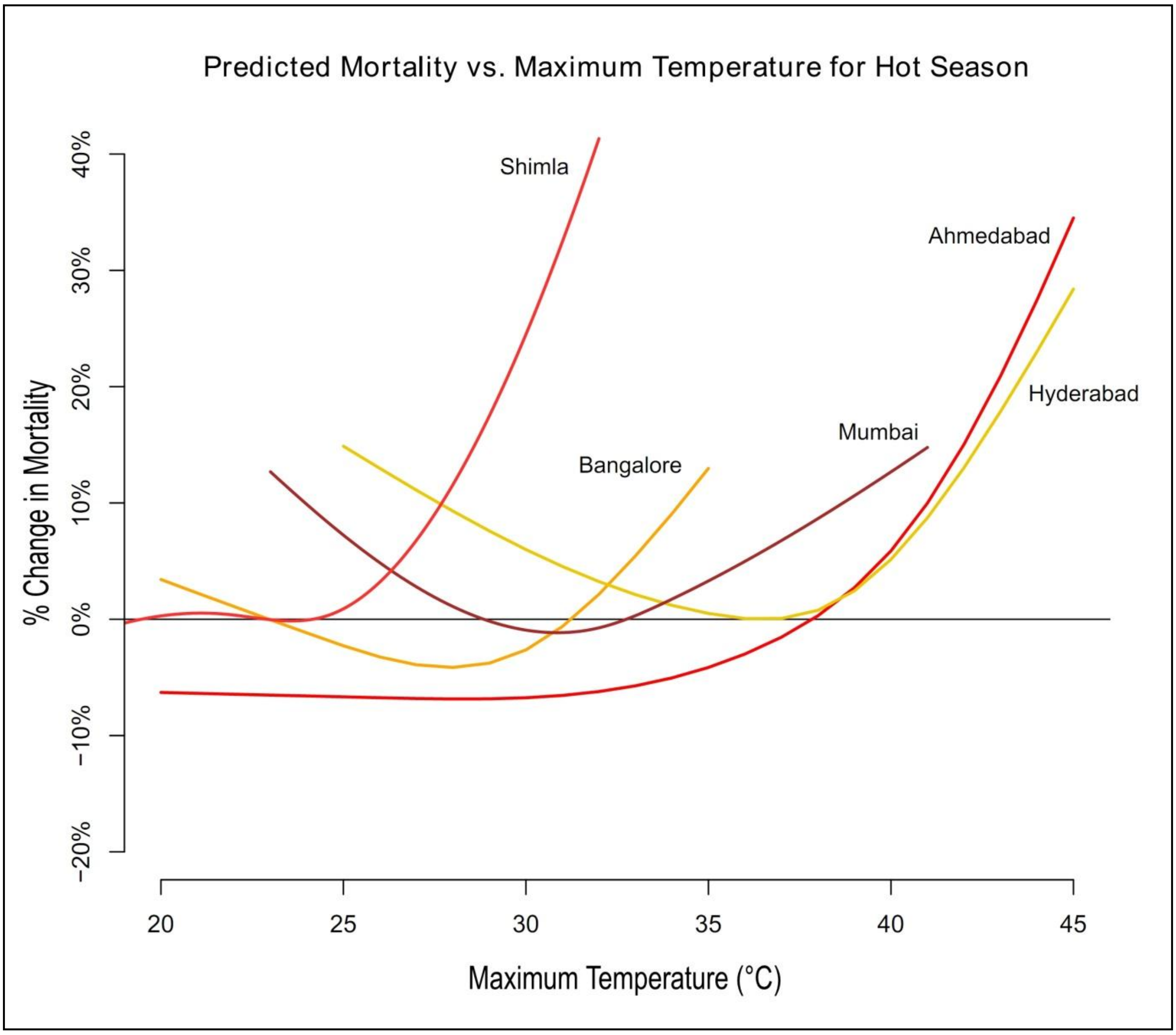

Figure S.2 Exposure response curves for summer season in representative cities. The x-axis shows the maximum temperature (°C). The y-axis shows the percentage increase in mortality relative to the minimum mortality temperature for each city. It is observed that the exposure response curves vary according to city.

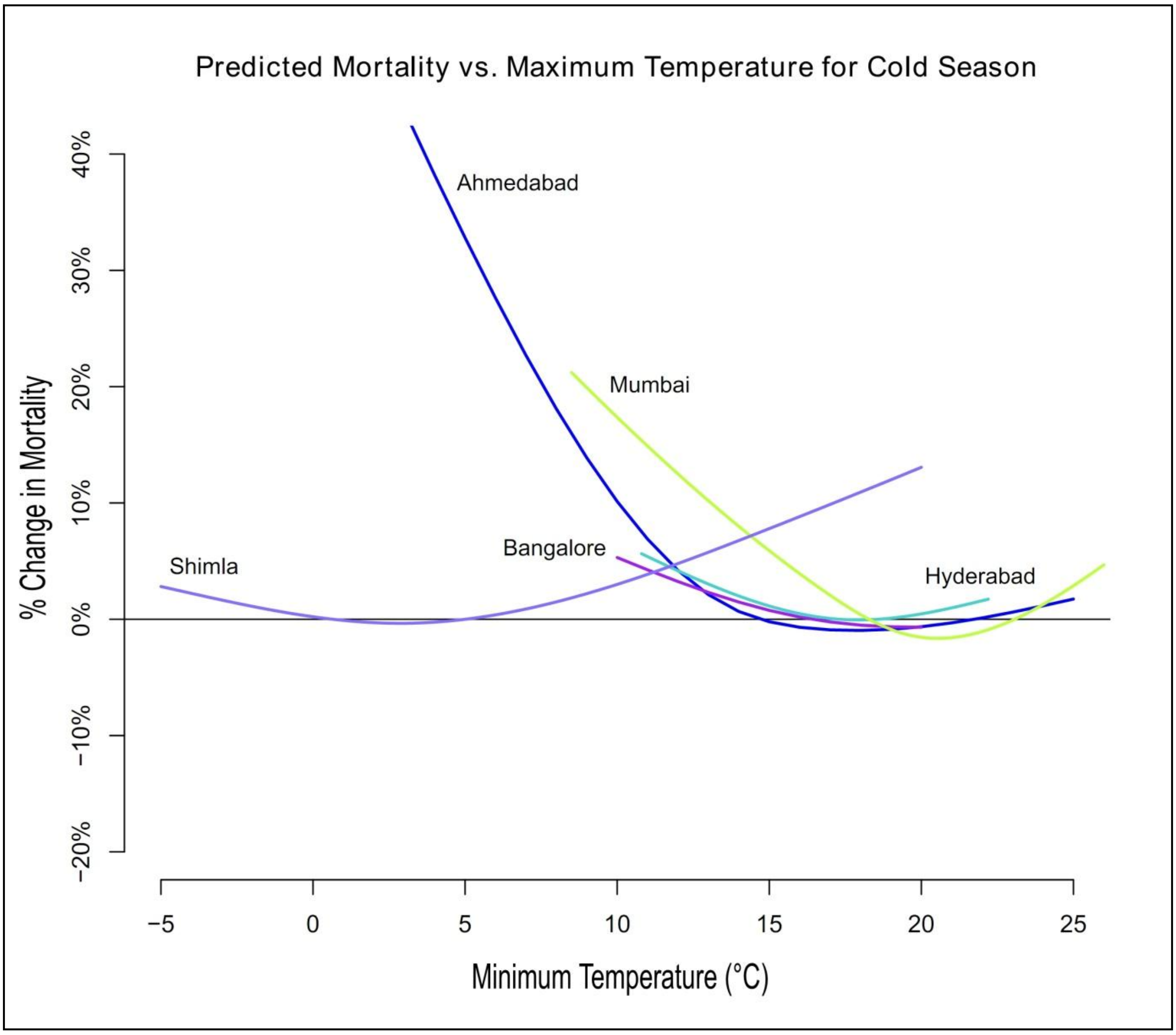

Figure S.3 Exposure response curves for winter season in representative cities. The x-axis shows the minimum temperature (°C). The y-axis shows the percentage increase in mortality relative to the minimum mortality temperature for each city. It is observed that the exposure response curves vary according to city.

Table S.6 Cities with million plus population in 2011 as per climate zone

Hot & Dry	Warm & Humid	Composite	Temperate	Cold
Ahmedabad	**Mumbai**	**Hyderabad**	**Bangalore**	**Shimla***
Aurangabad	Mallapuram	Agra		Srinagar
Jaipur	Kolkata	Ludhiana		
Jodhpur	Asansol	Amritsar		
Kota	Pune	Chandigarh		
Nashik	Thissur	Ghaziabad		
Rajkot	Kozhikode	Kanpur		
Surat	Kochi	Delhi		
Vadodara	Thiruvananthapuram	Lucknow		
	Kannur	Varanasi		
	Kollam	Meerut		
	Chennai	Allahabad		
	Coimbatore	Patna		
	Madurai	Jamshedpur		
	Tiruchirapalli	Dhanbad		
	Vishakhapatnam	Ranchi		
		Raipur		
		Durg - Bhilainagar		
		Indore		
		Bhopal		
		Jabalpur		
		Gwalior		
		Nagpur		
		Faridabad		

Notes: Cities in bold are the representative cities whose temperature mortality relationships were applied

*Shimla is the only non-million plus city

Table S.7 Future estimates of mortality for India for summer season across models

Model	Baseline	RCP 4.5				RCP 8.5			
				Acclimatization*				Acclimatization*	
	2000s	2050s	2080s	2050s	2080s	2050s	2080s	2050s	2080s
ACCESS1-0	152500	213400	269500	208800	259100	246300	332100	242400	322900
BNU-ESM	152700	209100	242800	204300	231500	267300	372400	263800	364000
CCSM4	153400	195800	228900	191000	215800	265800	350100	262200	340800
CESM1-BGC	165100	215300	239100	210300	226800	262000	328400	258100	318300
CESM1-CAM5	130500	220200	281200	215600	270700	269400	358100	265400	348900
CMCC-CM	147100	226000	276800	221300	264800	273700	419600	270100	411900
CNRM-CM5	149500	198400	224200	193700	211800	221800	291300	217500	280300
FGOALS-g2	140900	200100	197900	195200	184900	229700	251400	225600	240500
FIO-ESM	131500	222900	205900	217900	191500	242500	350000	237700	339600
GFDL-CM3	151200	266800	330200	262800	321900	300000	419800	296600	411800
GFDL-ESM2G	148100	229500	230900	224600	218500	240700	342700	236100	332200
GFDL-ESM2M	147900	240400	256000	236000	244300	241600	348300	236600	338000
GISS-E2-R	143200	188300	199400	182800	184300	207300	271500	202600	259100
IPSL-CM5A-LR	162800	249700	292900	245100	283100	289600	406600	285800	397800
IPSL-CM5A-MR	150900	228100	292200	222900	281900	261200	387600	257000	378800
IPSL-CM5B-LR	129300	180600	227900	174700	213600	215900	299500	211100	286400
MIROC-ESM-CHEM	140200	255900	295700	251500	285400	300700	438200	298100	431000
MIROC-ESM	139400	251300	281300	246800	269700	279100	419100	276100	412300
MIROC5	140600	212900	217200	207700	204100	210500	263000	205500	250200
MPI-ESM-LR	156100	263400	286700	259700	276900	293900	423300	290600	415100
MPI-ESM-MR	160300	250700	255100	246700	244300	262600	402500	259100	394300
MRI-CGCM3	129300	187600	225400	182400	212300	230000	302500	225500	290300
NorESM1-M	153200	203200	218100	197700	203000	233800	325600	229600	315000
Average	***146800***	***222200***	***251100***	***217400***	***239100***	***254100***	***352300***	***250100***	***342600***
SD	***10300***	***25400***	***36100***	***25900***	***37700***	***28300***	***55800***	***28800***	***57500***

*This denotes the percentage change in mortality as a result of acclimatization

Table S.8 Future estimates of mortality for India for winter season across models

Model	Baseline	RCP 4.5				RCP 8.5			
				Acclimatization				Acclimatization	
	2000s	**2050s**	**2080s**	**2050s**	**2080s**	**2050s**	**2080s**	**2050s**	**2080s**
ACCESS1-0	98400	69000	52900	65800	46300	53300	40300	50200	36300
BNU-ESM	94100	60700	54600	57400	45900	47800	23200	44500	17700
CCSM4	100500	79100	63200	75800	54600	61100	39900	57900	33800
CESM1-BGC	96400	79400	70100	76000	61400	58100	38400	54900	32300
CESM1-CAM5	101500	60000	48700	56800	40900	49300	23300	46000	19800
CMCC-CM	92400	57100	42500	53900	36200	44900	13900	42000	12100
CNRM-CM5	98200	75800	62200	72700	54700	71900	40800	68900	34800
FGOALS-g2	90900	57800	61500	54300	52900	49100	35100	46000	29300
FIO-ESM	94600	75800	65800	72500	57100	58100	39200	54800	33200
GFDL-CM3	96900	59400	44600	56400	38400	43200	21900	40800	19700
GFDL-ESM2G	94600	77600	72600	73900	63700	62300	34800	59100	28700
GFDL-ESM2M	94700	74200	68900	71000	60600	64600	34100	61400	28200
GISS-E2-R	95800	66400	59300	62800	51100	54600	32600	51400	26900
IPSL-CM5A-LR	95500	47500	42000	44700	36300	36800	16100	34800	13700
IPSL-CM5A-MR	89100	50200	34600	47300	28600	32000	12400	29500	9200
IPSL-CM5B-LR	100200	74300	66200	71200	59000	48000	27500	45400	23800
MIROC-ESM-CHEM	103700	60000	47800	56800	40300	47000	21000	44000	17000
MIROC-ESM	96200	67200	55300	63700	47200	50700	23700	47600	19000
MIROC5	93900	74500	56100	71200	48100	57900	39200	54600	32800
MPI-ESM-LR	88800	51300	49900	48300	42900	43800	21000	41200	17600
MPI-ESM-MR	93700	61100	51300	58100	43800	47300	21600	44400	18100
MRI-CGCM3	99900	71100	60700	67700	52800	62700	32700	59100	26900
NorESM1-M	98800	76000	77800	72800	70000	54300	43300	50900	36300
Average	***96000***	***66300***	***56900***	***63100***	***49300***	***52100***	***29400***	***49100***	***24700***
SD	***3810***	***9870***	***10890***	***9750***	***10200***	***9310***	***9550***	***9050***	***8290***

*This denotes the percentage change in mortality as a result of acclimatization

Table S.9 Future estimates of mortality for million plus cities for summer season

				RCP 4.5						RCP 8.5				
				Baseline			Acclimatization		Pop Inc*			Acclimatization		Pop Inc*
City	**Death rate**	**Population**	**Climate Zone**	**2000s**	**2050s**	**2080s**	**2050s**	**2080s**	**2080s**	**2050s**	**2080s**	**2050s**	**2080s**	**2080s**
Agra	6.1	1746467	Composite	2000	3000	3400	3000	3300	5100	3200	4300	3200	4200	6500
Allahabad	6.1	1216719	Composite	1500	2100	2400	2100	2300	3500	2400	3100	2400	3100	4600
Amritsar	5.6	1183705	Composite	600	1200	1400	1200	1400	2200	1400	2100	1400	2100	3200
Bhopal	6.1	1883381	Composite	1800	2700	3100	2700	3100	4300	3100	4300	3100	4300	5900
Chandigarh	4.1	1025682	Composite	100	300	400	300	400	600	400	800	400	800	1200
Delhi	4.3	16314838	Composite	9000	14500	16700	14500	16500	23100	16600	24200	16600	24000	33300
Dhanbad	5.2	1195298	Composite	400	800	1000	800	1000	1500	1000	1600	1000	1600	2500
Durg-Bhilai	6.1	1064077	Composite	1200	1700	1900	1700	1900	2900	2000	2600	2000	2600	4000
Faridabad	5.3	1404653	Composite	1100	1700	1900	1700	1900	2900	1900	2700	1900	2700	4100
Ghaziabad	6.1	1101981	Composite	1600	2600	3000	2600	2900	3000	2900	4300	2900	4200	4300
Gwalior	5.2	7749334	Composite	1300	2000	2200	2000	2200	3000	2100	2700	2100	2700	3600
Hyderabad	6.1	2167447	Composite	2800	6300	7700	6200	7500	9100	7900	12700	7900	12600	15000
Indore	5.2	1337131	Composite	2000	3200	3600	3200	3600	5100	3200	3600	3200	3600	7100
Jabalpur	6.1	1267564	Composite	1200	1800	2000	1800	2000	3000	2000	2800	2000	2800	4300
Jamshedpur	6.1	2920067	Composite	500	1000	1200	1000	1100	1700	1200	1800	1200	1800	2700
Kanpur	5.6	1613878	Composite	3500	5200	5800	5200	5800	9200	5600	7400	5600	7400	11700
Ludhiana	6.1	2901474	Composite	1200	2000	2300	2000	2300	3500	2000	2300	2000	2300	3500
Lucknow	6.1	1424908	Composite	2900	4500	5100	4500	5100	7000	5000	6900	5000	6800	9500
Meerut	5.1	2497777	Composite	1000	1700	2000	1700	2000	2900	2000	2900	2000	2900	4300
Nagpur	5.5	2046652	Composite	2600	3600	4100	3600	4000	5800	4100	5400	4100	5300	7700
Patna	6.1	1122555	Composite	700	1400	1800	1400	1700	2700	1800	3100	1800	3000	4800
Raipur	5.2	1126741	Composite	1300	1900	2100	1900	2000	2400	2200	2800	2200	2800	3300
Ranchi	6.1	1435113	Composite	300	700	800	700	800	1200	800	1400	800	1400	1900
Varanasi	6.1	2358525	Composite	1500	2300	2600	2300	2600	3600	2600	3500	2600	3500	4900
Ahmedabad	5.7	6352254	Hot & Dry	13600	22300	24700	22000	23900	30200	22000	31200	21700	30500	38100

Aurangabad	5.1	1189376	Hot & Dry	1900	2900	3300	2800	3200	4400	3400	4900	3400	4800	6600
Jaipur	5.8	3073350	Hot & Dry	6200	9300	10500	9100	10100	14500	10300	14400	10200	14100	20000
Jodhpur	5.8	1137815	Hot & Dry	2600	3900	4400	3900	4300	5900	4300	5900	4300	5800	7900
Kota	5.8	1001365	Hot & Dry	2300	3300	3700	3300	3600	4600	3700	5000	3600	4900	6300
Nashik	5.1	1562769	Hot & Dry	900	1500	1800	1300	1500	2500	1800	3100	1700	2900	4300
Rajkot	5.7	1390933	Hot & Dry	1200	2000	2400	1900	2100	3200	2400	3900	2200	3700	5300
Surat	5.7	4585367	Hot & Dry	4000	6600	7900	6200	7000	9700	7900	13000	7600	12400	16000
Vadodara	5.7	1817191	Hot & Dry	3100	4800	5500	4700	5300	5100	5500	8100	5400	7900	11600
Asansol	6.5	1243008	Warm & Humid	2200	2700	3000	2600	2900	3800	3000	3600	3000	3600	4600
Coimbatore	6.4	8696010	Warm & Humid	600	1100	1300	1000	900	1500	1500	2400	1300	2100	2800
Kochi	6.4	2151466	Warm & Humid	200	500	700	300	200	800	800	1600	600	1100	1700
Chennai	6.6	2117990	Warm & Humid	14300	18500	20100	18300	19300	23600	20700	25100	20500	24800	29400
Kolkata	6.5	14112536	Warm & Humid	17200	24300	27800	23600	25900	40500	28400	36600	27800	35600	53300
Madurai	5.1	18414288	Warm & Humid	600	1100	1400	1000	900	1700	1500	2300	1400	2000	2900
Mumbai	6.4	1462420	Warm & Humid	8000	12800	14800	12100	12600	21200	15500	23300	15000	22000	33400
Pune	5.1	5049968	Warm & Humid	4000	5600	6200	5500	5900	7900	6400	8900	6300	8600	11200
Tiruchirapalli	6.4	1021717	Warm & Humid	900	1400	1600	1400	1500	2300	1700	2400	1700	2300	3300
Vishakhapatanam	5.2	1730320	Warm & Humid	1600	2400	2600	2300	2400	3300	2600	3500	2600	3300	4400
Bhubhaneshwar	6.5	837737	Warm & Humid	700	1000	2000	900	1900	2100	1500	2000	1400	1900	3100
Kozhikode	6.6	2030519	Warm & Humid	300	700	900	500	400	600	1000	1800	800	1400	1200
Vijaywada	5.2	1491202	Warm & Humid	2000	2700	2900	2600	2800	3300	2900	3500	2900	3400	4000
Mallapuram	6.6	1698645	Warm & Humid	200	600	700	400	300	700	800	1500	700	1200	1500
Thrissur	6.6	1854783	Warm & Humid	200	600	800	400	300	800	900	1600	700	1300	1600
Vasai-Virar	5.1	1221233	Warm & Humid	500	800	1000	800	800	1000	1000	1500	1000	1500	1500
Bangalore	5.2	8499399	Temperate	13900	20100	22100	19900	21100	25200	23200	28800	23000	28000	32800
Shimla	3.6	169758	Cold	100	200	300	200	300	300	300	400	300	400	400
Srinagar	4.7	1273312	Cold	100	200	300	200	200	400	300	800	300	700	1000

Table S.10 Future estimates of mortality for million plus cities for winter season

		RCP 4.5						RCP 8.5				
		Baseline			**Acclimatization**		**Pop Inc***			**Acclimatization**		**Pop Inc***
City	Climate Zone	**2000s**	**2050s**	**2080s**	**2050s**	**2080s**	**2080s**	**2050s**	**2080s**	**2050s**	**2080s**	**2080s**
Agra	Composite	2390	1820	1650	1820	1640	2500	1490	930	1490	920	1410
Allahabad	Composite	1270	920	800	920	800	1200	720	390	720	390	590
Amritsar	Composite	2120	1680	1540	1680	1540	2400	1480	980	1480	980	1530
Bhopal	Composite	1580	1010	820	1010	810	1140	730	330	730	310	460
Chandigarh	Composite	1410	1100	1010	1100	1010	1430	960	630	960	630	900
Delhi	Composite	17160	13060	11790	13050	11750	16270	10970	6900	10970	6840	9530
Dhanbad	Composite	790	540	430	540	430	660	390	190	380	180	290
Durg-Bhilai	Composite	470	260	190	260	180	280	170	50	160	40	80
Faridabad	Composite	1770	1340	1210	1340	1200	1840	1120	700	1120	690	1060
Ghaziabad	Composite	3040	2310	2090	2310	2080	2390	1940	1220	1940	1210	1400
Gwalior	Composite	1450	1090	980	1090	970	1300	890	540	890	530	720
Hyderabad	Composite	1010	400	280	390	230	330	230	60	220	40	70
Indore	Composite	1790	1120	900	1110	880	1250	750	1180	750	1170	1640
Jabalpur	Composite	1130	750	620	750	610	940	560	260	560	250	390
Jamshedpur	Composite	710	450	360	450	350	530	310	140	310	130	200
Kanpur	Composite	3610	2700	2410	2700	2400	3790	2170	1290	2170	1270	2020
Ludhiana	Composite	2600	2000	1820	2000	1820	2700	1740	1120	1740	1110	1650
Lucknow	Composite	3340	2510	2240	2500	2230	3080	1970	1180	1970	1160	1620
Meerut	Composite	2110	1610	1450	1610	1450	2120	1340	850	1340	840	1240
Nagpur	Composite	1050	590	430	580	410	610	390	130	390	110	180
Patna	Composite	1520	1020	870	1020	860	1350	770	420	770	410	650
Raipur	Composite	510	270	200	270	190	230	180	50	180	40	60
Ranchi	Composite	860	590	490	590	480	670	440	220	440	210	300
Varanasi	Composite	1450	1030	900	1030	890	1230	790	430	790	420	600
Ahmedabad	Hot & Dry	1490	690	430	590	230	520	360	100	280	40	120

Aurangabad	Hot & Dry	150	60	40	50	10	50	30	10	20	0	10
Jaipur	Hot & Dry	2440	1640	1350	1600	1220	1880	1200	550	1160	410	760
Jodhpur	Hot & Dry	730	460	360	450	300	470	310	120	290	80	170
Kota	Hot & Dry	520	310	240	300	190	300	210	80	190	50	100
Nashik	Hot & Dry	210	80	50	60	20	70	40	10	30	0	10
Rajkot	Hot & Dry	240	100	60	80	30	80	50	10	40	0	20
Surat	Hot & Dry	330	110	60	70	20	80	50	10	30	0	10
Vadodara	Hot & Dry	270	110	70	80	30	2500	60	10	40	0	20
Asansol	Warm & Humid	1630	1360	1220	1310	1070	1550	1140	760	1080	580	970
Coimbatore	Warm & Humid	480	190	120	80	10	140	90	10	30	0	20
Kochi	Warm & Humid	0	0	0	0	0	0	0	0	0	0	0
Chennai	Warm & Humid	410	100	60	20	0	70	40	10	10	0	10
Kolkata	Warm & Humid	12940	9640	8330	8890	6230	12150	7630	4280	6860	2380	6230
Madurai	Warm & Humid	0	0	0	0	0	0	0	0	0	0	0
Mumbai	Warm & Humid	11300	7070	5610	5840	2720	8040	5010	1830	3810	550	2620
Pune	Warm & Humid	3920	2740	2310	2450	1470	2930	2130	940	1800	400	1190
Tiruchirapalli	Warm & Humid	0	0	0	0	0	0	0	0	0	0	0
Vishakhapatanam	Warm & Humid	440	200	140	120	30	180	120	30	60	0	30
Bhubhaneshwar	Warm & Humid	450	270	220	220	100	340	190	80	140	20	120
Kozhikode	Warm & Humid	260	80	40	20	0	30	30	0	10	0	0
Vijaywada	Warm & Humid	270	100	60	50	10	70	50	10	30	0	10
Mallapuram	Warm & Humid	220	70	40	20	0	40	30	0	10	0	0
Thrissur	Warm & Humid	20	0	0	0	0	0	0	0	0	0	0
Vasai-Virar	Warm & Humid	750	470	370	390	180	370	330	120	250	40	120
Bangalore	Temperate	380	110	70	70	10	80	50	10	30	0	10
Shimla	Cold	3	1	1	1	0	0	1	0	0	0	0
Srinagar	Cold	320	210	180	210	180	230	160	80	160	80	100

Uncertainty analysis (estimates across 23 models)

Table S.11 shows the mean and standard deviation of future estimates across different models

	Summer					Winter				
		RCP 4.5		RCP 8.5			RCP 4.5		RCP 8.5	
Models	**Baseline**	**2050s**	**2080s**	**2050s**	**2080s**	**Baseline**	**2050s**	**2080s**	**2050s**	**2080s**
ACCESS1-0	152500	213400	269500	246300	332100	98400	69000	52900	53300	40300
BNU-ESM	152700	209100	242800	267300	372400	94100	60700	54600	47800	23200
CCSM4	153400	195800	228900	265800	350100	*100500*	79100	63200	61100	39900
CESM1-BGC	*165100*	215300	239100	262000	328400	96400	79400	70100	58100	38400
CESM1-CAM5	130500	220200	281200	269400	358100	101500	60000	48700	49300	23300
CMCC-CM	147100	226000	276800	273700	419600	92400	57100	42500	44900	13900
CNRM-CM5	149500	198400	224200	221800	291300	98200	75800	62200	71900	40800
FGOALS-g2	140900	200100	197900	229700	251400	90900	57800	61500	49100	35100
FIO-ESM	131500	222900	205900	242500	350000	94600	75800	65800	58100	39200
GFDL-CM3	151200	266800	330200	300000	419800	96900	59400	44600	43200	21900
GFDL-ESM2G	148100	229500	230900	240700	342700	94600	77600	72600	62300	34800
GFDL-ESM2M	147900	240400	256000	241600	348300	94700	74200	68900	64600	34100
GISS-E2-R	143200	188300	199400	207300	271500	95800	66400	59300	54600	32600
IPSL-CM5A-LR	*162800*	249700	292900	289600	406600	95500	47500	42000	36800	16100
IPSL-CM5A-MR	150900	228100	292200	261200	387600	89100	50200	34600	32000	12400
IPSL-CM5B-LR	129300	180600	227900	215900	299500	100200	74300	66200	48000	27500
MIROC-ESM-CHEM	140200	255900	295700	300700	438200	*103700*	60000	47800	47000	21000
MIROC-ESM	139400	251300	281300	279100	419100	96200	67200	55300	50700	23700
MIROC5	140600	212900	217200	210500	263000	93900	74500	56100	57900	39200
MPI-ESM-LR	156100	263400	286700	293900	423300	88800	51300	49900	43800	21000
MPI-ESM-MR	*160300*	250700	255100	262600	402500	93700	61100	51300	47300	21600
MRI-CGCM3	129300	187600	225400	230000	302500	99900	71100	60700	62700	32700

NorESM1-M	153200	203200	218100	233800	325600	98800	76000	77800	54300	43300
µ (Mean)	***146800***	***222200***	***251100***	***254100***	***352300***	***96000***	***66300***	***56900***	***52100***	***29400***
σ (SD)	***10300***	***25400***	***36100***	***28300***	***55800***	***3800***	***9900***	***10900***	***9300***	***9500***

Cells with *italics* fill indicate three highest estimates of summer baseline and winter baseline mortality respectively

Of the models used in the analysis, those that provide the three highest estimates of summer baseline mortality include the CESM-M1-BGC, IPSL-CM5A-LR and MPI-ESM-MR (Table S.11). Correspondingly, those models that show the highest increases in winter baseline mortality include the CCSM4, CESM1-CAM5 and MIROC-ESM-CHEM.

Table S.12 shows the percentage change in morality estimates across different models

	Summer				**Winter**			
	RCP 4.5		**RCP 8.5**		**RCP 4.5**		**RCP 8.5**	
Models	**2050s**	**2080s**	**2050s**	**2080s**	**2050s**	**2080s**	**2050s**	**2080s**
ACCESS1-0	39.9%	76.7%	61.5%	117.8%	-29.9%	-46.2%	-45.8%	-59.0%
BNU-ESM	36.9%	59.0%	75.0%	143.9%	-35.5%	-42.0%	-49.2%	-75.3%
CCSM4	27.6%	49.2%	73.3%	128.2%	-21.3%	-37.1%	-39.2%	-60.3%
CESM1-BGC	30.4%	44.8%	58.7%	98.9%	-17.6%	-27.3%	-39.7%	-60.2%
CESM1-CAM5	68.7%	115.5%	106.4%	174.4%	-40.9%	-52.0%	-51.4%	-77.0%
CMCC-CM	53.6%	88.2%	86.1%	***185.2%***	-38.2%	-54.0%	-51.4%	*-85.0%*
CNRM-CM5	32.7%	50.0%	48.4%	94.8%	-22.8%	-36.7%	-26.8%	***-58.5%***
FGOALS-g2	42.0%	40.5%	63.0%	*78.4%*	-36.4%	-32.3%	-46.0%	-61.4%
FIO-ESM	69.5%	56.6%	84.4%	166.2%	-19.9%	-30.4%	-38.6%	-58.6%
GFDL-CM3	76.5%	118.4%	98.4%	177.6%	-38.7%	-54.0%	-55.4%	-77.4%
GFDL-ESM2G	55.0%	55.9%	62.5%	131.4%	-18.0%	-23.3%	-34.1%	-63.2%

GFDL-ESM2M	62.5%	73.1%	63.4%	135.5%	-21.6%	-27.2%	-31.8%	-64.0%
GISS-E2-R	31.5%	39.2%	44.8%	*89.6%*	-30.7%	-38.1%	-43.0%	-66.0%
IPSL-CM5A-LR	53.4%	79.9%	77.9%	149.8%	-50.3%	-56.0%	-61.5%	*-83.1%*
IPSL-CM5A-MR	51.2%	93.6%	73.1%	156.9%	-43.7%	-61.2%	-64.1%	*-86.1%*
IPSL-CM5B-LR	39.7%	76.3%	67.0%	131.6%	-25.8%	-33.9%	-52.1%	-72.6%
MIROC-ESM-CHEM	82.5%	110.9%	114.5%	***212.6%***	-42.1%	-53.9%	-54.7%	-79.7%
MIROC-ESM	80.3%	101.8%	100.2%	***200.6%***	-30.1%	-42.5%	-47.3%	-75.4%
MIROC5	51.4%	54.5%	49.7%	*87.1%*	-20.7%	-40.3%	-38.3%	***-58.3%***
MPI-ESM-LR	68.7%	83.7%	88.3%	171.2%	-42.2%	-43.8%	-50.7%	-76.4%
MPI-ESM-MR	56.4%	59.1%	63.8%	151.1%	-34.8%	-45.3%	-49.5%	-76.9%
MRI-CGCM3	45.1%	74.3%	77.9%	134.0%	-28.8%	-39.2%	-37.2%	-67.3%
NorESM1-M	32.6%	42.4%	52.6%	112.5%	-23.1%	-21.3%	-45.0%	***-56.2%***
μ (Mean)	***51.7%***	***71.5%***	***73.5%***	***140.4%***	***-31.0%***	***-40.8%***	***-45.8%***	***-69.5%***
σ (SD)	***16.8%***	***24.5%***	***19.0%***	***37.1%***	***9.5%***	***11.0%***	***9.2%***	***9.7%***

Cells with ***bold & italics*** indicate three highest percentage increases in the summer and winter season under RCP 8.5 in 2080s
Cells with *underline and italics* indicate three lowest percentage increases in the summer and season under RCP 8.5 in 2080s

The percentage changes in the mortality estimates by model are provided in Table S.12. For the summer season, the highest percentage changes in estimates are observed for models CMCC-CM, MIROC-ESM-CHEM and MIROC-ESM under RCP 8.5 scenario in the 2080s. Correspondingly the models that show the least percentage changes for summer season are FGOALS-g2, GISS-E2-R and MIROC5.

For the winter season, the highest percentage declines are shown by models IPSL-CM5A-LR, IPSL-CM5A-MR and CMCC-CM under the RCP 8.5 scenario in 2080s. The models that show the least percentage decline in mortality estimates for the winter season are NorESM1-M, MIROC5 and CNRM-CM5.

References – Supplementary material

Anderson, B. G., & Bell, M. L. (2009). Weather-Related Mortality: How Heat, Cold, and Heat Waves Affect Mortality in the United States. *Epidemiology*, *20*(2), 205–213. doi:10.1097/EDE.0b013e318190ee08

Anderson, G. B., & Bell, M. L. (2011). Heat waves in the United States: mortality risk during heat waves and effect modification by heat wave characteristics in 43 US communities. *Environmental health perspectives*, *119*(2), 210.

Barnett, A. G., Hajat, S., Gasparrini, A., & Rocklöv, J. (2012). Cold and heat waves in the United States. *Environmental Research*, *112*, 218–224. doi:10.1016/j.envres.2011.12.010

Bhaskaran, K., Gasparrini, A., Hajat, S., Smeeth, L., & Armstrong, B. (2013). Time series regression studies in environmental epidemiology. *International Journal of Epidemiology*. doi:10.1093/ije/dyt092

Dholakia H. H., Bhadra, D., & Garg, A. (2014). Short term association between ambient air pollution and mortality and modification by temperature in five Indian cities. *Atmospheric Environment*, *99*, 168–174.

Hajat, S., Kovats, R. S., & Lachowycz, K. (2006). Heat-related and cold-related deaths in England and Wales: who is at risk? *Occupational and Environmental Medicine*, *64*(2), 93–100. doi:10.1136/oem.2006.029017

Li, T., Horton, R. M., & Kinney, P. L. (2013). Projections of seasonal patterns in temperature- related deaths for Manhattan, New York. *Nature Climate Change*. doi:10.1038/nclimate1902

RGI. (2012). *Sample Registration System Bulletin 2011* (No. 47). New Delhi: Registrar General of India.

Rocklov, J., Barnett, A. G., & Woodward, A. (2012). On the estimation of heat-intensity and heat-duration effects in time series models of temperature-related mortality in Stockholm, Sweden. *Environmental Health*, *11*(1), 1–12.

WHO. (2010). *International Classification of Diseases - 10*. Geneva: World Health Organization. Retrieved from http://apps.who.int/classifications/icd10/browse/2010/en